Supporting Information

B-O Covalent Bonds Annulated Hot Exciton Molecular Design for High-Performance Narrowband UV-OLEDs

Jie Li,[a] Zhang-Li Cheng, [b] Yue Wang,[a] Shu-Qi Zhang,[b] Hui Wang,[b] Ling-Wei Qu,[a] Mai Ke Lin,[a] Xi Zhang,[a] Jia Yu,[b] Bin Chen ,*[a] Kai Wang,*[b,c] Jun Ye*[a]

[a] School of Materials Science and Chemical Engineering, Ningbo University, Ningbo, Zhejiang, 315211, P. R. China

[b] Institute of Functional Nano & Soft Materials (FUNSOM), Soochow University, Suzhou, Jiangsu, 215123, P. R. China

[c] State Key Laboratory of Bioinspired Interfacial Materials Science, Soochow University, Suzhou, Jiangsu, 215123, P. R. China

*Corresponding authors: chenbin2@nbu.edu.cn; wkai@suda.edu.cn; yejun@nbu.edu.cn.

General information

Synthesis. The chemicals and reagents purchased from commercial sources were used without further purification unless otherwise stated. The main synthesis was performed using standard Schlenk techniques under a nitrogen atmosphere, and the target molecules were further purified by sublimation. ^{1}H NMR spectra were measured on a Bruker 400 MHz spectrometer with tetramethylsilane (TMS) as the internal standard. Mass analyses were recorded by an Autoflex MALDI-TOF mass spectrometer. Elemental analysis was performed using a Vario Micro cube.

Theoretical calculation. The front molecular orbitals (FMOs) of the optimized ground state and excited state were calculated with time-dependent density functional theory (TD-DFT) employing the B3LYP/6-31g(d) basis set in the Gaussian 16 program package. Natural transition orbital (NTO) analysis and determination of the contributions of atoms to FMOs were carried out using a multifunctional wavefunction analyzer (Multiwfn 3.6).

Electrochemical measurements. Cyclic voltammetry (CV) was performed on a CHI660e electrochemistry station. The samples were all prepared in *N,N*-dimethylformamide solution and degassed with nitrogen gas for 10 minutes before the test. The supporting electrolyte was 0.1 M tetrabutylammonium hexafluorophosphate ($[nBu_4N]PF_6$), while the gold, platinum and 3.0 M $Ag/AgNO_3$ electrodes served as the working, counter and reference electrodes, respectively. Cyclic voltammograms were obtained at a scan rate of 0.02 $V \cdot s^{-1}$ with standardization against ferrocene/ferrocenium.

Photophysical measurements. UV–vis absorption and photoluminescence (PL) spectra were recorded by using a Hitachi ultraviolet–visible (UV–vis) spectrophotometer U-3010 and a Hitachi fluorescence spectrometer F-4600, respectively. The PL quantum efficiency (PLQY) was measured via an absolute PL quantum yield measurement system (C11347-01, Hamamatsu Photonics) under a flow of nitrogen gas with an excitation wavelength of 300 nm. Transient decay measurements were carried out with an Edinburgh fluorescence spectrometer (FLS920).

Analysis of rate constants. The key kinetic parameters of the two emitters are estimated according to the following equations[1-2]:

$$\varphi_{total} = \varphi_p + \varphi_d \qquad \varphi_T = 1-\varphi_p$$

$$k_p = \frac{1}{\tau_p} \qquad k_d = \frac{1}{\tau_d}$$

$$k_r^S = k_p\varphi_p \qquad k_{ISC} = k_p(1-\varphi_p)$$

$$k_{RISC} = \frac{k_p k_d \varphi_d}{k_{ISC}\varphi_p} \qquad k_{nr}^T = k_d - \left(1-\frac{k_{ISC}}{k_p}\right)k_{RISC}$$

where φ_p and φ_d are the prompt and delayed fluorescence quantum efficiencies, respectively; φ_T is the ISC efficiency; and k_p, k_{RISC}, and k_d are the rate constants of prompt fluorescence, the RISC, and delayed fluorescence decay, respectively. k_r^S and k_{nr}^T are the rate constants of the singlet radiative transition and triplet nonradiative transition, respectively.

Device fabrication and measurement of EL characteristics. OLEDs were fabricated on indium tin oxide (ITO)-coated transparent glass substrates with multiple layers. The ITO glass substrates had a thickness of ca. 100 nm and a sheet resistance of ca. 30 Ω per square and were cleaned with an optical detergent, deionized water, acetone, and isopropanol successively and then dried in an oven. For vacuum-evaporation OLEDs, the ITO substrates were first exposed to UV ozone for 15 minutes. All the organic materials were thermally evaporated at a rate of 1 Å s^{-1} under a vacuum of ca. 10^{-5} Torr. Finally, LiF and Al were successively deposited at rates of 0.1 Å s^{-1} and 5 Å s^{-1}, respectively. Four identical OLED devices were formed on each of the substrates, and the emission area was 0.09 cm^2 for each device. For solution-processed OLEDs, the ITO substrates were first exposed to UV ozone for 15 minutes. The EL performances of the devices were measured with a PHOTO RESEARCH Spectra Scan PR 655 PHOTOMETER and a KEITHLEY 2400 Source Meter constant current source at room temperature.

Experimental

Synthesis

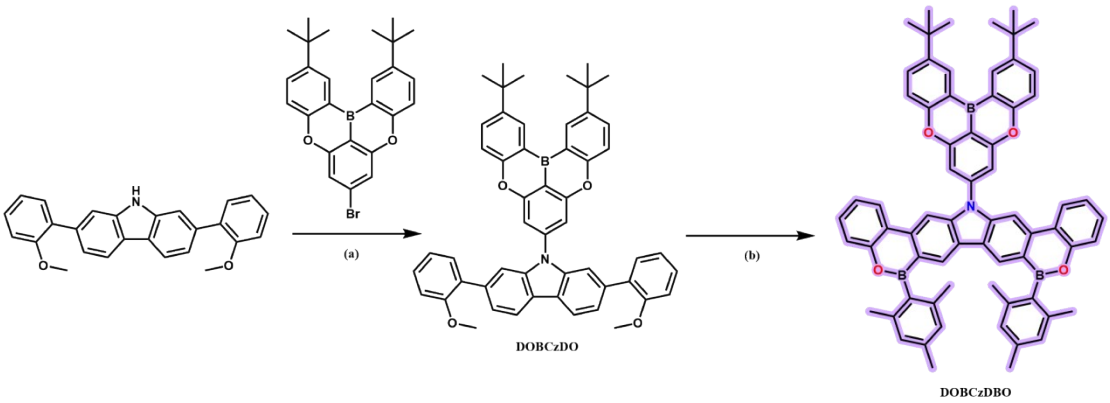

Scheme S1 Synthetic routes of **DOBCzDO** and **DOBCzDBO**. Reaction conditions: (a) $Pd(OAc)_2$, $[(tBu)_3P]HBF_4$, *t*-BuONa, toluene, 110 °C; (b) Mesitylene, RT; BBr_3, -20 °C; DIEA, 150 °C; MesMgBr, RT.

Synthesis of DOBCzDO：

A mixture of 7-bromo-2,12-di-tert-butyl-5,9-dioxa-13b-boranaphtho [3,2,1-de]anthracene (4.61 g, 10 mmol), 3,6-Bis(2-methoxyphenyl)-9H-carbazole (3.79 g, 11 mmol), $Pd_2(dba)_3$ (0.45 g, 0.5 mmol), $[(tBu)_3P]HBF_4$ (0.29 g, 1 mmol), *t*-BuONa (1.92 g, 20 mmol) and 50 ml toluene were added in a 100 mL two-necked round-bottom flask refluxed at 110 °C under N_2 protection for 12 hours. After cooling to room temperature, the mixture was extracted with water (3 × 50 mL) and dichloromethane (DCM, 3 × 50 mL) for three times. The organic layer was dried over anhydrous magnesium sulfate ($MgSO_4$), filtered, and then the solvent was evaporated. The residue was purified via column chromatography eluting with petroleum ether: dichloromethane (5:1, V/V) to obtain a green solid (5.67 g, yield: 71%). ^1H NMR (400 MHz, Chloroform-*d*). δ 8.80 (d, J = 2.4 Hz, 2H), 8.21 (d, J = 8.1 Hz, 2H), 7.96 – 7.91 (m, 2H), 7.81 (dd, J = 8.8, 2.4 Hz, 2H), 7.58 – 7.50 (m, 6H), 7.47 (dd, J = 7.5, 1.6 Hz, 2H), 7.37 – 7.32 (m, 2H), 7.09 – 7.01 (m, 4H), 3.89 (s, 6H), 1.53 (s, 18H). $C_{52}H_{46}BNO_4$(C, 83.39; H, 6.19; N, 1.87). HR-MS (m/z): calcd for $C_{52}H_{46}BNO_4$ 759.1855; Found 759.1868.

Synthesis of DOBCzDBO:

Under a nitrogen atmosphere, BBr_3 (1.2 mL, 10 mmol) was added dropwise in a solution of **DOBCzDO** (1.51 g, 2 mmol) in *o*-dichlorobenzene (30 mL) at room temperature. The reaction mixture was stirred at room temperature for 3.0 h. Then, N, N-diisopropylethylamine (DIEA) (0.53 mL, 3.0 mmol) was added at 0 °C, and the reaction mixture was allowed to warm to 150 °C for 12 h. After cooling to room temperature, MesMgBr (18 mL, 15 mmol) was added, and the reaction mixture was allowed to warm to 50 °C for 2 h. The mixture was extracted with water (3 × 50 mL) and dichloromethane (DCM, 3 × 50 mL) for three times. The organic layer was dried over anhydrous magnesium sulfate ($MgSO_4$), filtered, and then the solvent was evaporated. The residue was purified by column chromatography eluting with petroleum ether: dichloromethane (2:1, V/V) to afford **DOBCzDBO** (1.24 g, yield: 84%). ^{1}H NMR (400 MHz, Chloroform-*d*) δ 8.91 (d, J = 2.5 Hz, 2H), 8.72 (s, 2H), 8.45 (s, 2H), 8.29 (dd, J = 8.3, 1.6 Hz, 2H), 7.91 (dd, J = 8.8, 2.4 Hz, 2H), 7.65 (s, 1H), 7.63 (d, J = 2.0 Hz, 3H), 7.57 (dd, J = 8.1, 1.3 Hz, 2H), 7.47 (ddd, J = 8.2, 7.1, 1.5 Hz, 2H), 7.34 – 7.29 (m, 2H), 7.04 (s, 4H), 2.45 (s, 6H), 2.29 (s, 12H), 1.59 (s, 18H). $C_{68}H_{60}B_3NO_4$(C, 85.50 H, 6.33; N,1.47) HR-MS (m/z): calcd for $C_{68}H_{60}B_3NO_4$ 989.4933; Found 987.4940

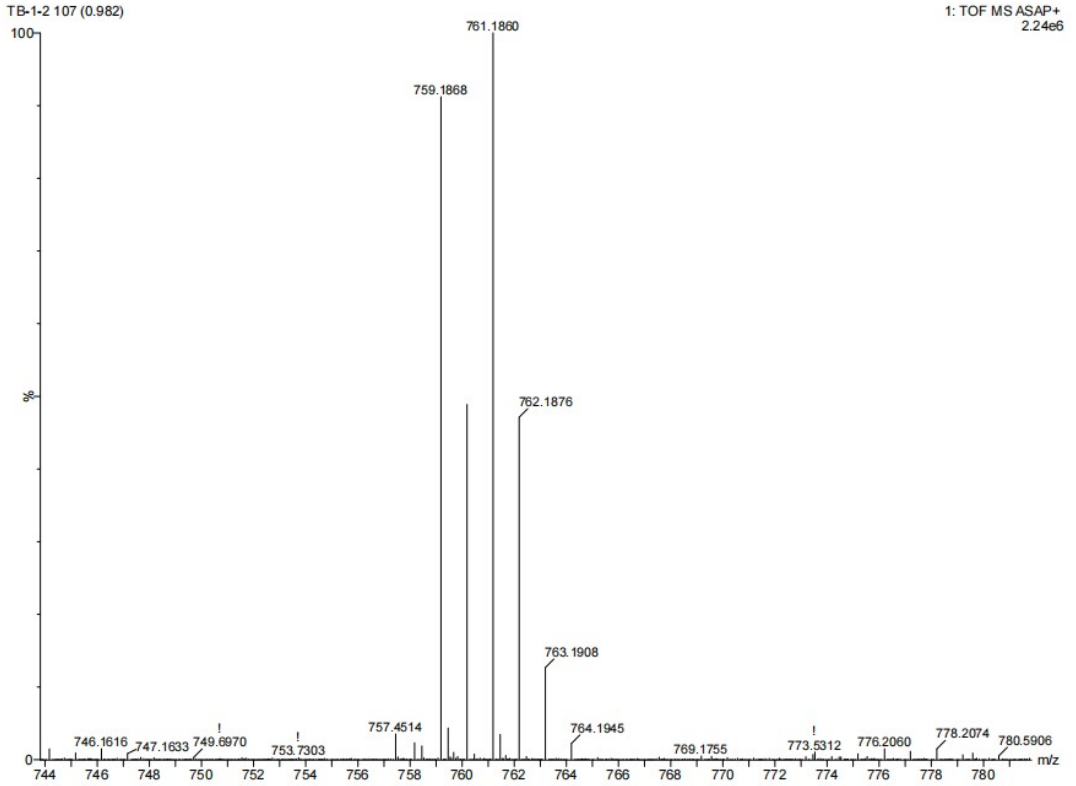

Figure S1. High-resolution mass spectrum (HRMS) of **DOBCzDO**.

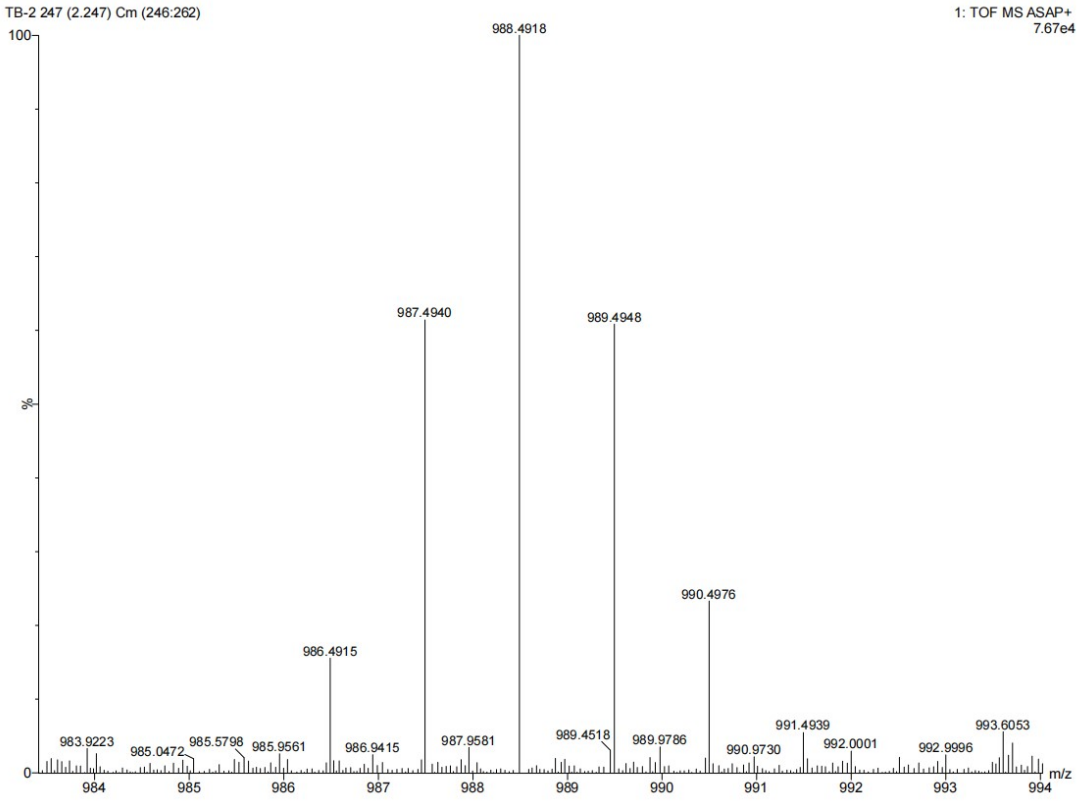

Figure S2. High-resolution mass spectrum (HRMS) of **DOBCzDBO**.

Thermostability

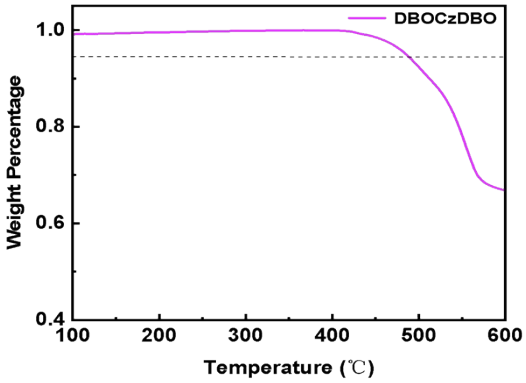

Figure S3. TGA curve of **DOBCzDBO**.

Electrochemical properties

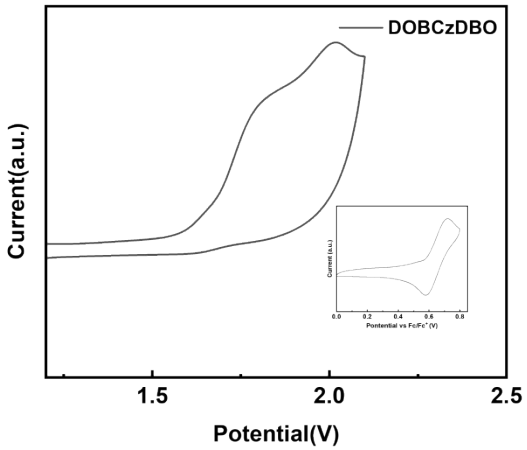

Figure S4. Cyclic voltammogram curve of **DOBCzDBO**.

Theoretical calculations

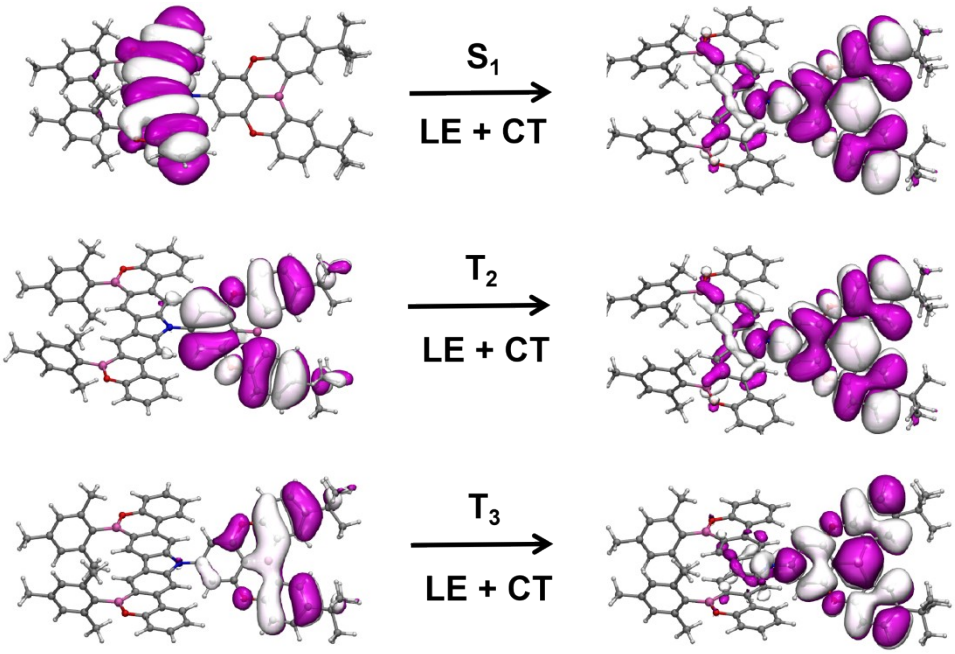

Figure S5. The natural transition orbits (NTOs) analysis of **DBOCzDBO**.

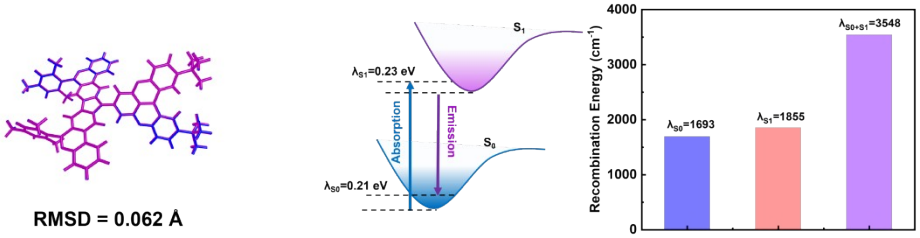

Figure S6. Reorganization energies with optimized S_0 and S_1 geometries and single point energies of **DBOCzDBO,** and geometry comparison between optimized S_0 (blue) and S_1 (purple) states of **DBOCzDBO.**

Photophysical properties

Table S1. Kinetic parameters of **DOBCzDBO**.

Emitters	λ_{abs}[a] [nm]	λ_{PL}[b] [nm]	Φ_{PLQY}[c] [%]	τ_{PL}[d] [ns]	HOMO[e] [eV]	LUMO[f] [eV]	E_{opt}[g] [eV]	T_d[h] [°C]
DOBCzDBO	362	391	70.4	6.01	-6.05	-2.56	3.4	489

a Maximum absorption wavelength in dilute toluene solutions (10^{-5} mol L^{-1}).
b Measured in dilute toluene solutions.
c Measured in 2 wt% **DOBCzDBO** doped mCP film.
d Fluorescence lifetimes in tetrahydrofuran.
e Measured by cyclic voltammetry measurement.
f LUMO = HOMO + E_{opt}
g Optical energy gap obtained from the onset of UV-vis absorption spectrum in toluene.
h Decomposition temperature (5% weight loss).

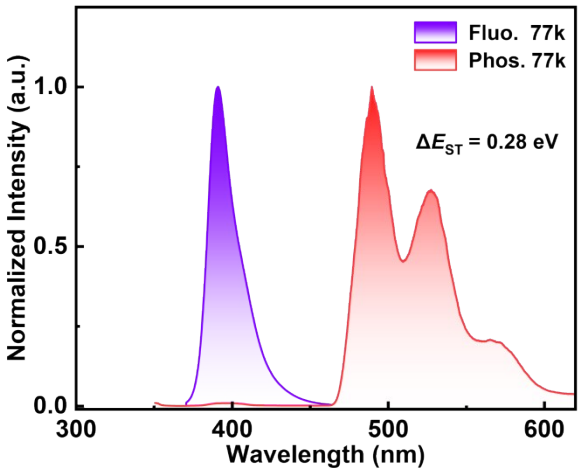

Figure S7. Normalized fluorescence and phosphorescence spectra of 2 wt% **DOBCzDBO** based mCP thin films at 77K.

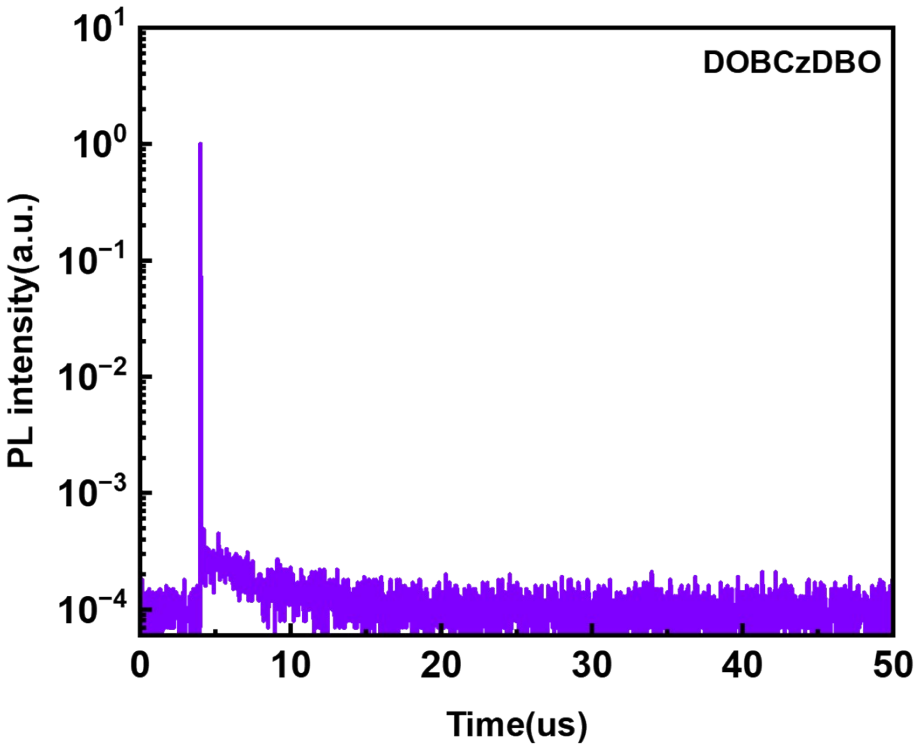

Figure S8. The transient PL decay curves of **DOBCzBO** in toluene solution (10^{-5} M).

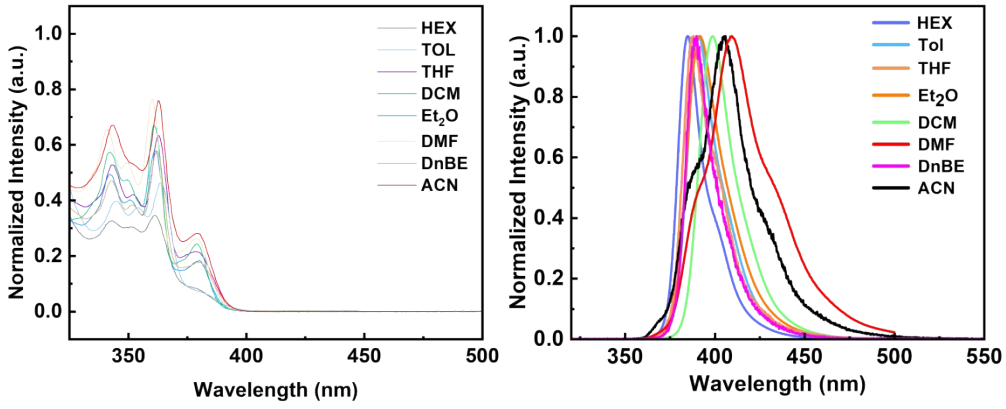

Figure S9. a) UV–Vis absorption of **DOBCzDBO**, and b) emission spectra **DOBCzDBO** in various solvents at room temperature.

Table S2. Summary of the EL data of **DOBCzDBO** at different doping ratios.

Compound	Doped [wt%]	λ_{EL} [a] [nm]	FWHM [b] [nm]	EQE_{max} [c] [%]	CE_{max} [d] [cd m^{-2}]	PE_{max} [e] [lm W^{-1}]	CIE [f] (x,y)
DOBCzDBO	1	391	24	5.9	1.8	1.1	(0.16,0.02)
	2	391	28	8.9	2.3	1.8	(0.16,0.02)
	3	393	29	3.8	0.9	0.8	(0.16,0.02)
	10	394	33	4.3	1.3	1.0	(0.16,0.03)

[a] Peak wavelength of the EL spectrum; [b] Full width at half maximum; [c] Maximum external quantum efficiency; [d] Maximum current efficiency; [e] Maximum power efficiency; [f] Commission Internationale de l'Elcairage (CIE) coordinates.

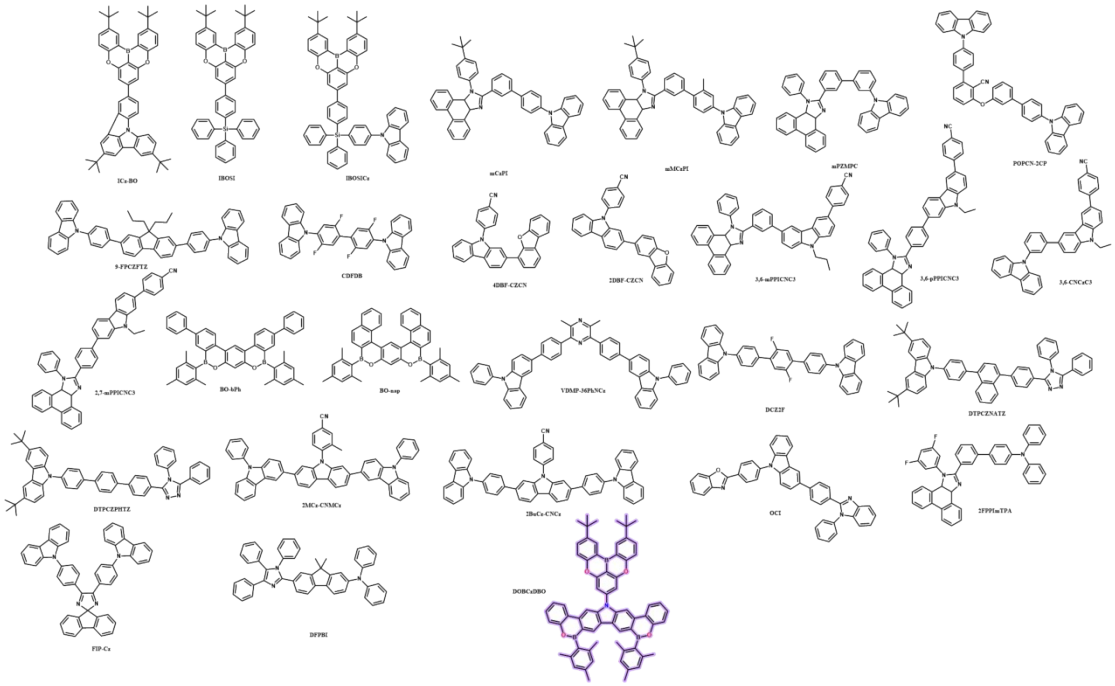

Figure S10. Chemical structures of hot exciton emitters ($CIE_\gamma < 0.046$).

Table S3. Device Performances Comparison for hot exciton emitters ($CIE_\gamma < 0.046$).

Compound	λ_{EL}[a] [nm]	FWHM[b] [nm]	EQE_{max}[c] [%]	CIE (x, y) [d]	Ref.
DOBCzDBO	**392**	**28**	**8.9**	**(0.162, 0.020)**	**This work**
ICz-BO	**414**	**37**	**12.01**	**(0.164, 0.031)**	**[1]**
9-PCZCFTZ	**390**	**-**	**14.5**	**(0.162, 0.045)**	**[2]**
CDFDB	**398**	**55**	**12.0**	**(0.16, 0.04)**	**[3]**
4DBF-CZCN	**390**	**42**	**3.00**	**(0.164, 0.034)**	**[4]**
2DBF-CZCN	**388**	**38**	**2.86**	**(0.164, 0.036)**	
3,6-CNCzC3	**407**	**44**	**6.69**	**(0.161, 0.028)**	**[5]**
3,6-mPPICNC3	**391**	**41**	**7.85**	**(0.161, 0.025)**	**[6]**
3,6-pPPICNC3	**406**	**41**	**7.51**	**(0.160, 0.035)**	
2,7-mPPICNC3	**425**	**51**	**5.42**	**(0.161, 0.033)**	
BO-bph	**394**	**48**	**11.3**	**(0.166, 0.021)**	**[7]**
BO-Nap	**404,421**	**45**	**11.9**	**(0.161, 0.022)**	
mCzPI	**376,395**	**38**	**3.78**	**(0.165, 0.028)**	**[8]**
mMCzPI	**376,393**	**38**	**3.03**	**(0.166, 0.027)**	
FIP-CZ	**427**	**49**	**10.40**	**(0.158, 0.039)**	**[9]**
VDMP-36PhCz	**404**	**50**	**7.55**	**(0.159, 0.039)**	**[10]**
tBOSi	**414**	**32**	**9.15**	**(0.165, 0.034)**	**[11]**
tBOSiCz	**414**	**32**	**8.91**	**(0.163, 0.031)**	
DCZ2F	**404**	**50**	**5.62**	**(0.163, 0.035)**	**[12]**
DTPCZNATZ	**427**	**-**	**4.4**	**(0.157, 0.035)**	**[13]**
DTPCZPHTZ	**427**	**-**	**5.7**	**(0.157, 0.037)**	
2MCz-CNMCz	**404**	**-**	**7.76**	**(0.158, 0.039)**	
mP2MPC	**376, 395**	**51**	**6.09**	**(0.163, 0.028)**	**[14]**
POPCN-2CP	**388**	**40**	**5.3**	**(0.161, 0.025)**	**[15]**
2BuCz-CNCz	**396**	**33**	**10.79**	**(0.161, 0.031)**	**[16]**

OCI	**424**	**55**	**5.06**	**(0.158, 0.036)**	**[17]**
2FPPI mTPA	**416**	**-**	**4.12**	**(0.160, 0.038)**	**[18]**
DFPBI	**425**	**56**	**4.96**	**(0.157, 0.039)**	**[19]**

[a] Peak wavelength of the EL spectrum; [b] Full width at half maximum; [c] Maximum EQE; [d] Commission Internationale de l'Elcairage (CIE) coordinates.

NMR spectra

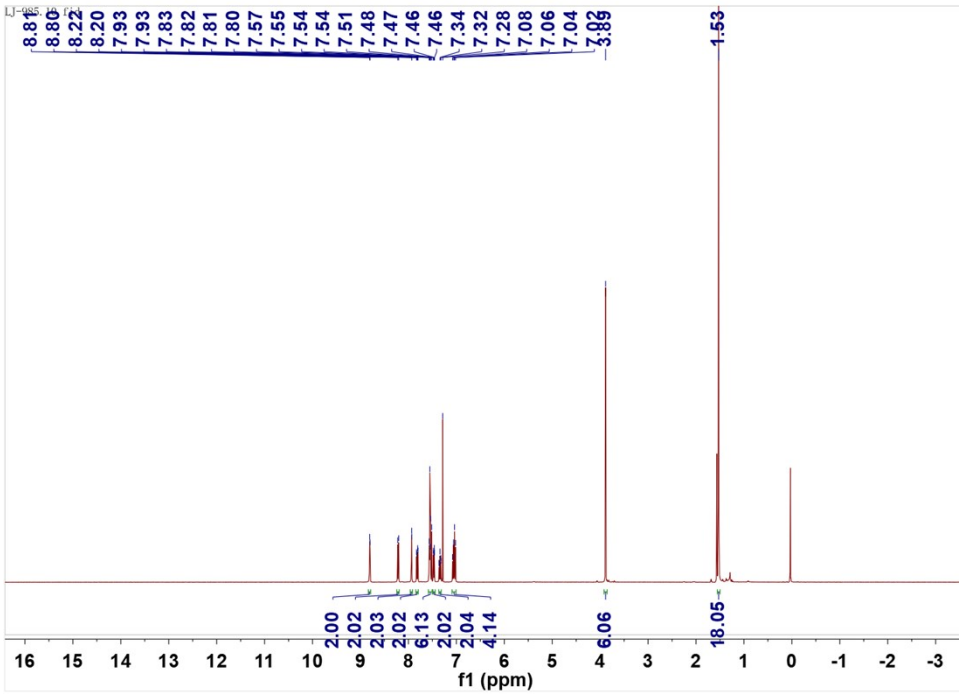

Figure S11. ^{1}H NMR spectrum ($CDCl_3$, 400 MHz) of **DOBCzDO**.

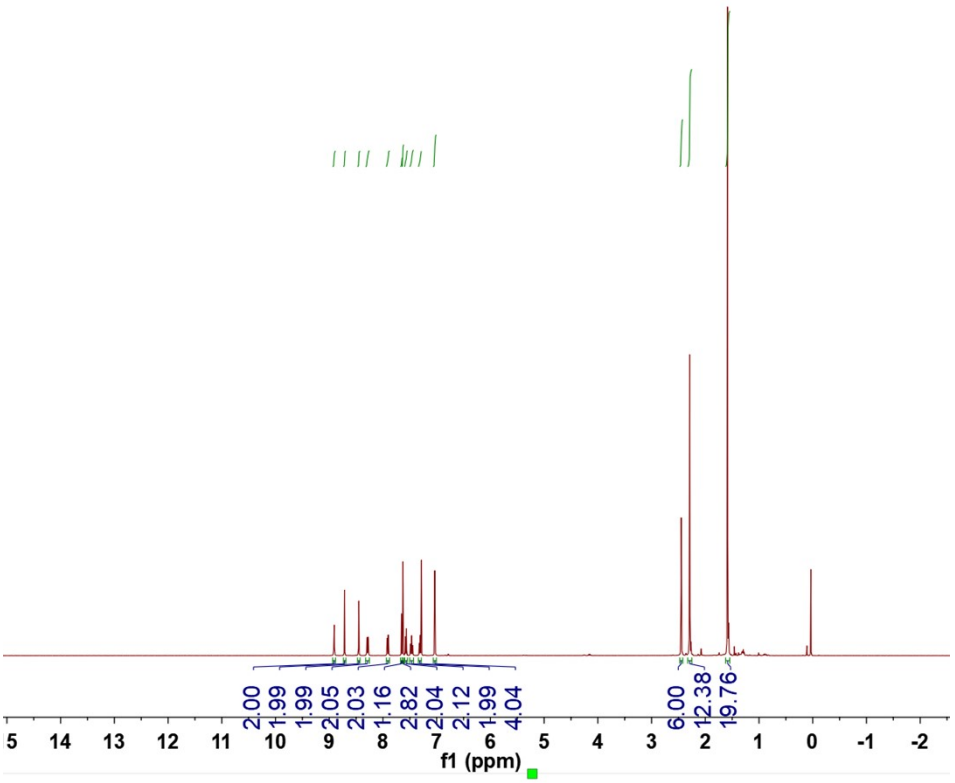

Figure S12. ^{13}H NMR spectrum ($CDCl_3$, 400 MHz) of **DOBCzDBO**.

Reference

[1] H. Zhou, R. Wang, M. Sun, Y. Zhou, L. Zhang, J. Song, Q. Sun, S.-T. Zhang, W. Yang, S. Xue, *Chem. Sci.* **2024**, 15, 18601–18607.

[2] K. Zhang, Z. Zhou, D. Liu, Y. Chen, S. Zhang, J. Pan, X. Qiao, D. Ma, S. Su, W. Zhu, Y. Liu, *Angew. Chem. Int. Ed.* **2024**, 63, e202407502.

[3] H. Huang, R. Chen, S. He, S. Wang, H. Qi, L. Peng, Y. Liu, S. Ying, S. Yan, *Dyes Pigm.* **2024**, 231, 112420.

[4] H. Qi, S. Wang, Z. Gao, D. Xie, J. Li, Y. Liu, S. Xue, S. Ying, D. Ma, S. Yan, *ACS Mater. Lett.* **2024**, 6, 3844–3853.

[5] H. Qi, D. Xie, Z. Gao, S. Wang, L. Peng, Y. Liu, S. Ying, D. Ma, S. Yan, *Chem. Sci.* **2024**, 15, 11053–11064.

[6] G. Li, K. Xu, J. Zheng, X. Fang, W. Lou, F. Zhan, C. Deng, Y.-F. Yang, Q. Zhang, Y. She, *J. Am. Chem. Soc.* **2024**, 146, 1667–1680.

[7] Z. Zhong, Z. Liu, X. Wang, D. Xiong, H. Li, X. J. Feng, Z. Zhao, H. Lu, *J. Mater. Chem. C* **2023**, 11, 16271–16279.

[8] C. Liao, B. Chen, Q. Xie, X. Li, H. Liu, S. Wang, *Adv. Mater.* **2023**, 35, 2305310.

[9] T. Chen, J. Lou, H. Wu, J. Luo, D. Yang, X. Qiao, H. Zhang, B. Z. Tang, Z. Wang, *Adv. Opt. Mater.* **2023**, 11, 2301053.

[10] X.-Q. Gan, Z.-M. Ding, D.-H. Liu, W.-Q. Zheng, B. Ma, H. Zhang, X. Chang, L. Wang, Y. Liu, X. Wu, S.-J. Su, W. Zhu, *Adv. Opt. Mater.* **2023**, 11, 2300195.

[11] Y. Huo, J. Lv, M. Wang, Z. Duan, H. Qi, S. Wang, Y. Liu, L. Peng, S. Ying, S. Yan, *J. Mater. Chem. C* **2023**, 11, 6347–6353.

[12] M. Sun, T. Li, M. Xie, H. Zhou, Q. Sun, D. Liu, Y. Pan, S. Zhang, W. Yang, S. Xue, *Dyes Pigm.* **2023**, 210, 111002.

[13] X. Guo, G. Li, J. Lou, K. Chen, R. Huang, D. Yang, H. Zhang, Z. Wang, B. Z. Tang, *Small* **2022**, 18, 2204029.

[14] L. Peng, J. Lv, S. Xiao, Y. Huo, Y. Liu, D. Ma, S. Ying, S. Yan, *Chem. Eng. J.* **2022**, 450, 138339.

[15] J. Chen, H. Liu, J. Guo, J. Wang, N. Qiu, S. Xiao, J. Chi, D. Yang, D. Ma, Z. Zhao, B. Z. Tang, *Angew. Chem. Int. Ed.* **2022**, 61, e202116810.

[16] H. Zhang, G. Li, X. Guo, K. Zhang, B. Zhang, X. Guo, Y. Li, J. Fan, Z. Wang, D. Ma, B. Z. Tang, *Angew. Chem. Int. Ed.* **2021**, 60, 22241–22247.

[17] H. Zhou, M. Yin, Z. Zhao, Y. Miao, X. Jin, J. Huang, Z. Gao, H. Wang, J. Su, H. Tian, *J. Mater. Chem. C* **2021**, 9, 5899–5907.

[18] Z. Li, N. Xie, Y. Xu, C. Li, X. Mu, Y. Wang, *Org. Mater.* **2020**, 02, 011–019.

[19] X. Qiu, S. Ying, C. Wang, M. Hanif, Y. Xu, Y. Li, R. Zhao, D. Hu, D. Ma, Y. Ma, *J. Mater. Chem. C* **2019**, 7, 592–600.